PII: S0955-2219(98)00112-5

0955-2219/98/$—see front matter

Microstructure Effects in the X-ray Powder Diffraction Profile of 9 mol% Mg-PSZ

F. L. Cumbrera,[a]* F. Sanchez-Bajo,[b] R. Fernández[c] and L. Llanes[c]

[a]Departamento de Física, Facultad de Ciencias, Universidad de Extremadura. Avda. de Elvas s/n, 06071 Badajoz, Spain
[b]Departamento de Electrónica e Ingeniería Electromecánica, Escuela de Ingenierías Industriales, Universidad de Extremadura, Ctra de Olivenza s/n. Badajoz, Spain
[c]Departamento de Ciencia de los Materiales e Ingeniería Metalúrgica. E.T.S.I.I.B. (UPC). Avda. Diagonal, 647. 08028 Barcelona, Spain

(Received 23 January 1998; revised version received 31 March 1998; accepted 9 April 1998)

Abstract

The relative abundances of the polymorphs present in samples of 9 mol% magnesia-partially stabilized zirconia (Mg-PSZ) have been determined by Rietveld analysis of X-ray powder diffraction data. The composition of the samples is mainly dominated by the tetragonal content. Preferred orientation and anisotropic line broadening effects on this majority phase were observed. It is shown that the consideration of these microstructural effects during the Rietveld refinement is not only important with the aim of improving the refinement but also indispensable to obtain the accurate proportion of the phases. © *1998 Elsevier Science Limited. All rights reserved*

1 Introduction

The most interesting properties of zirconia based ceramics are certainly found within the class of alloys known as partially stabilized zirconias (PSZ). One of the most widely studied ceramic material in this class is the magnesia-partially-stabilized zirconia (Mg-PSZ). Thus, it has been shown[1] how by the careful choice of thermal treatment cycles the mechanical properties of Mg-PSZ may be tailored so as to make the material suitable for relevant applications. The relative abundance of its polymorphs: cubic (c), tetragonal (t), monoclinic (m), orthorombic (o) and the δ phase, $Mg_2Zr_5O_{12}$, have been determined for several compositions by Rietveld analysis of X-ray and neutron powder diffraction data.[2–5] Early, the most common means of obtaining quantitative information from diffraction data was the so-called polymorph method.[6] However, some difficulties including the strong peak overlap in a mixture of polymorphs and the occurrence of extinction and preferred orientation effects[7,8] brought about the decline of this procedure. In practice, the only net result was the measurement of the monoclinic content.[9] More recently, Caracoche *et al.*[10] have shown, by means of the time-differential perturbed-angular-correlation (TDPAR) technique, the existence of a high-MgO-content nontransformable t′ phase. The presence of this t′ phase has frequently been reported for the Y-PSZ system[11–14] but only exceptionally quoted for magnesia-doped zirconia.[10] On the other hand, Ikuma *et al.*[15] have studied, by means of scanning and transmission electron microscopy (SEM and TEM), the grain size of the polymorphic phases of the $MgO–ZrO_2$ system depending on temperature and several additive concentrations.

In all PSZ materials the t-phase is dispersed as precipitates within a stabilized cubic matrix. In fact, the main aim in the fabrication of this kind of toughened ceramics is to develop the t-phase into a metastable state in such a way that martensitic transformation to monoclinic phase can be readily stress-induced. This transformation is accompanied by a 3% volume increase which diminishes the crack tip opening (stress) and hence, induces a higher crack growth resistance. The morphology of tetragonal precipitates in PSZ materials has been studied by means of TEM by Bansal and Heuer[16] and Lanteri *et al.*[17] The habit plane and the corresponding morphology depend on the nature of the stabilizer: Mg, Ca, Y..., etc. This dependence arises because of differences in lattice parameters between the tetragonal precipitate and the cubic matrix.

*To whom correspondence should be addressed.

Thus, for the Mg-PSZ system, the precipitates form as oblate ellipsoids (disk-like) with an aspect ratio close to 5. Although the exact habit plane is irrational, it is close to {001}, the fourfold ⟨001⟩ direction being the rotation axis of the ellipsoid (both, plane and axis referred to the face-centered pseudocubic cell). These morphologic features have been explained in terms of anisotropic elasticity using the theory of Khachaturyan.[18] In fact the equilibrium shape of the precipitate represents a compromise between interfacial and strain energies.

It is noteworthy to remark that these morphologic features of the tetragonal precipitates have exclusively been investigated by means of TEM and electron diffraction experiments. Obviously, the study of these geometric aspects by means of X-ray diffraction experiments can yield very useful data as far as concerning with a volume-weighted information (within several micrometers of the surface) versus the strictly local information supplied by electron microscopy. From a theoretical viewpoint, at least two kinds of effects would be discernible on the X-ray profile of the tetragonal phase. They are related to the preferential orientation of the precipitates as well as to the anisotropic broadening of Bragg reflections due to its disk-shaped morphology. With respect to previous papers (i.e. Refs 2 and 4) preferred orientation corrections were applied in the Rietveld refinement, but only for the monoclinic contribution. On the other hand, the relatively high values for the agreement factors in these papers (about 10% and more, for R_{wp}) clearly suggest that significative microstructure effects in the tetragonal phase have been overlooked. In this letter, the above effects are considered during the Rietveld refinement of the diffraction pattern of a peak-aged 9 mol% Mg-PSZ sample. We have shown the real importance of these factors allowing us:

(a) to investigate microstructural features and improving the final quality of the refinement, and
(b) to obtain more accurate phase abundances; in practice, it is shown that the neglect of this subtle effects can yield misleading results, i.e. the tetragonal phase is overestimated at the expense of the monoclinic one.

2 Experimental Details and Procedures

The sample of Mg-PSZ chosen for study was a commercial product (9 mol% MgO, Friedrichsfeld Germany) supplied as a rectangular prism $5\times8\times50\,mm^3$. For X-ray data collection, a foil of thickness about 1·5 mm was cut from the prism. The powder X-ray diffraction (XRD) data were collected with a Philips PW-1800 diffractometer fitted with an automatic step-scanning system and graphite monochromator, and operating at 40 kV and 30 mA. The wavelength was the corresponding to the K_α radiation of Cu ($\lambda = 0{\cdot}15483$ nm). The data were collected over the 2θ range 15 to 136° at intervals of 0·02° 2θ using a step-counting time of 10 s.

For TEM observations thin foils were cut and mechanically ground to 100 μm. Disks (3 mm diameter) were then cut from the foils using an ultrasonic drill. The disks were afterward dimpled to 30 μm and ion milled. A thin film of carbon was evaporated onto the foil to avoid charging under the electron beam. Finally, a 120 kV JEOL 1200EXII electron microscope was used for TEM observations.

The profile refinements were performed with a version of the Rietveld analysis program FULLPROF.[19] The modified Thompson–Cox–Hastings pseudo-Voigt function was assumed as profile function. Starting values for the structure parameters were taken from previous refinements of Mg-PSZ samples.[24] The relative abundance of polymorphs was determined from the scale factors obtained at the completion of Rietveld refinement and using the simple relation of Hill and Howard.[2] Starting with a conventional refinement protocol, which takes into account structural, profile and global parameters,[20] in subsequent iterations microstructure effects were assumed by applying preferred orientation corrections and considering anisotropic broadening for Bragg peaks. Because preferred orientation produces systematic distortions of the reflection intensities, a scattering-matter-conserving preferred orientation correction based on the March–Dollase function[21] was applied

$$P = G_2 + (1 - G_2)\left(G_1^2 \cos^2\alpha + (1/G_1)\sin^2\alpha\right)^{-3/2} \quad (1)$$

where G_1 is a refinable parameter related to the nature of the habit (plate-like, needle-like..., etc.), G_2 is another refinable parameter representing the fraction of the sample that is not textured, and α is the acute angle between the scattering vector and the preferred orientation direction.

For an idealized structure with isotropic broadening, the full-width-at-half-maximum intensity, Γ, has frequently been modelled according to a modified version of the Caglioti expression[22]

$$\Gamma_G = \left\{U{\cdot}\tan^2\theta + V{\cdot}\tan\theta + W + Z/\cos^2\theta\right\}^{1/2} \quad (2)$$

$$\Gamma_L = X \cdot \tan\theta + Y/\cos\theta \qquad (3)$$

where U, V, W, Z, X and Y are refinable parameters and Γ_G and Γ_L are, respectively, the gaussian and lorentzian components of Γ.

In real materials, microstructure effects frequently gives rise to anisotropic broadening, and a smooth variation of Γ with 2θ cannot be expected. In practice, this effect may be clearly detected if the scatter in the Γ versus 2θ representation is larger than would be expected on statistical grounds. The actual version of FULLPROF[19] has implemented a microstructural model where anisotropic size effects can be modelled. For the case of a platelet habit, the lorentzian component of Γ is modified according to:

$$\Gamma_L = X \cdot \tan\theta + (Y + F(SZ))/\cos\theta \qquad (4)$$

where

$$F(SZ) = SZ \cdot \cos\psi \qquad (5)$$

in which SZ is a refinable parameter and ψ is the acute angle between the scattering vector and the vector defining the normal to the plate. The success of this rigorous treatment proved quite spectacular when it was applied to several troublesome problems.[23,24] In practice, however, anisotropy of breadth is usually ignored and an overall trend is considered in modelling the breadth variation.

3 Results and Discussion

In Fig. 1 the plot output for the first Rietveld analysis is shown, where microstructure effects on the tetragonal phase have not been taken into account. The lower curve is the difference between the observed and calculated intensity at each step, plotted on the same scale. It is worth noting that misfits in this difference plot correspond to the position of tetragonal reflections associated with reciprocal lattice directions:

(a) parallel to the rotation axis of the ellipsoid ([001]) or,
(b) perpendicular to [001], then contained in the equatorial plane of the oblate ellipsoid.

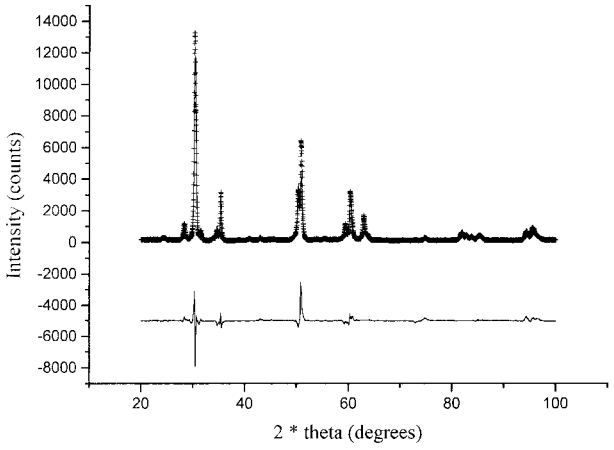

Fig. 1. Rietveld plot of refinement results for the case where preferred orientation and anisotropic broadening effects, for the t-phase, are not taken into account. Experimental data are given as crosses, whereas the calculated intensity and difference plots are plotted as solid lines on the same scale.

The calculated phase abundances and χ^2 residual are shown in Table 1. The studied material is essentially a binary mixture of tetragonal and cubic phases, whereas monoclinic phase is present at a level of about 15 wt%. These proportions are in good agreement with previous studies.[25] The orthorombic and rhombohedric polymorphs are absent in the studied samples since these phases will only be generated, respectively, on the application of stress or after aging at subeutectoid temperatures.[26–28] On the other hand, it is well known that the presence of the δ phase (which is formed at the expense of the cubic one) is associated with a drastic reduction of the abundance of the cubic matrix. In any case, it must be emphasized that the high value for the χ^2 factor is a strong indication that everything is not going well during the refinement. In Fig. 2, which is a bright-field TEM micrograph showing a typical pattern of tetragonal precipitates in the cubic matrix, the morphological features of the material, associated to the preferred orientation and characteristic disk-like shape, are evident. Indeed, Fig. 3 displays the variation of ($^\circ 2\theta$) with 2θ for reflections of the tetragonal phase. The severe scatter is a strong indication of a selective line broadening; an arrow indicates the most narrow reflection, which is associated to the [110] direction lying within the equatorial plane of the ellipsoid.

The next approach attempt to incorporate, during the final steps of the refinement, the influence of preferred orientation for the tetragonal precipitates. In doing so, the [001] direction was

Table 1. Weight fractions for the component phases, χ^2 agreement index, preferred orientation and anisotropic broadening parameters, for the Rietveld refinement strategies used in this work: (1) without considering preferred orientation and anisotropic broadening effects for the t-phase; (2) including preferred orientation effects in the [001] direction; (3) including plate-like anisotropic broadening effects; (4) including simultaneously both microstructural effect types

	t	c	m	χ^2	G_1	SZ
1	56·7	28·3	15·0	13·0	—	—
2	52·1	29·2	18·7	5·56	0·547	—
3	52·8	32·0	15·2	9·91	—	−0·0196
4	52·1	29·1	18·8	5·09	0·547	−0·0318

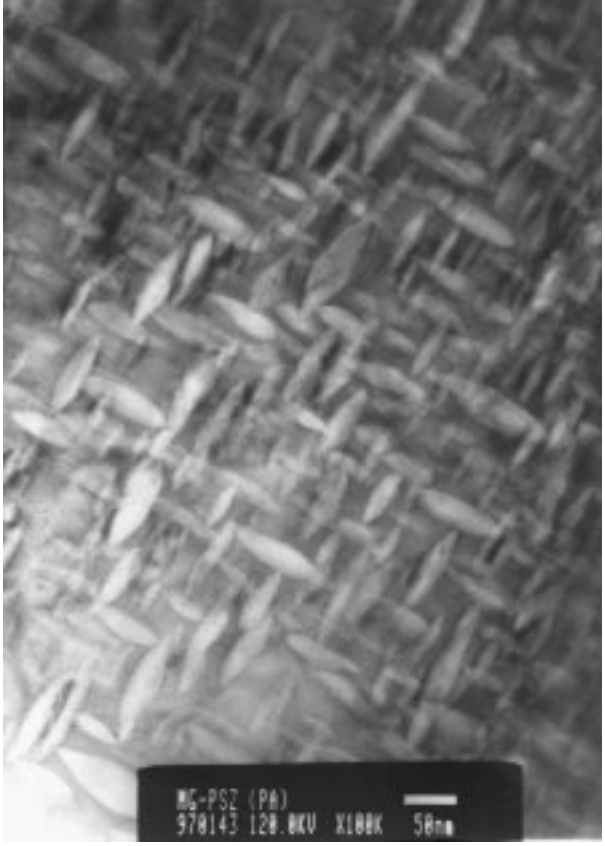

Fig. 2. Bright-field TEM micrograph of tetragonal precipitates in 9 mol% Mg-PSZ.

adopted as the preferred direction in reciprocal space. Figure 4 displays the Rietveld profile fit including the difference pattern. Note the remarkable improvement with respect to Fig. 1. In Table 1 it is observed a drastic reduction of the χ^2 factor from 13·0 to 5·56. The obtained value for the G_1 parameter in the March–Dollase function ($G_1 < 1$) indicates a platey habit for the tetragonal precipitates. At all events, the most interesting result concerns to the reduction (about 3·5 wt%) of the proportion of tetragonal phase, then increasing the monoclinic content.

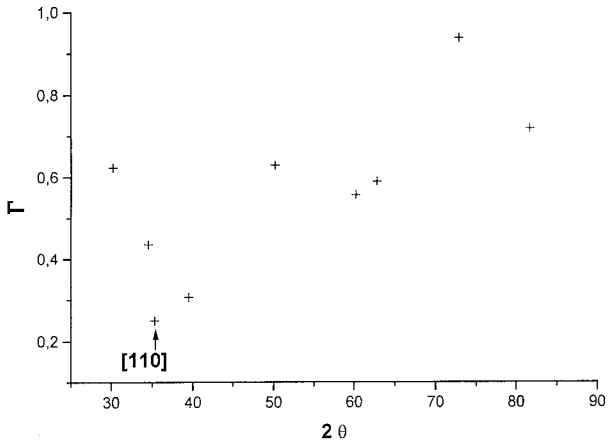

Fig. 3. Variation of Γ≡FWHM (°2θ) with 2θ for *hkl* diffraction lines of the tetragonal phase.

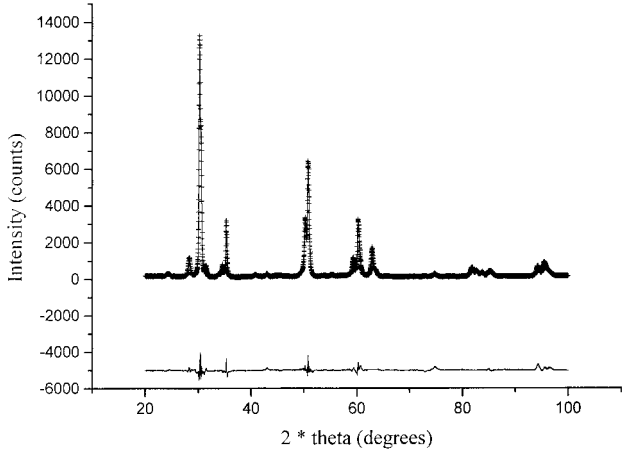

Fig. 4. Rietveld profile fit similar to that in Fig. 1, but including preferred orientation corrections for the tetragonal phase.

Going further it is now attempted to investigate the influence of anisotropic broadening on the tetragonal pattern. Figure 5 shows the corresponding Rietveld refinement plot. From the results collected in Table 1 it is readily shown a small improvement: the χ^2 factor is reduced from 13·0 to 9·91. This improvement is also evident after the observation of the difference plot in Fig. 5. Note that, in this case, the modification of phase abundances involves a switch from tetragonal to cubic.

Examination of Figs 1, 4 and 5 allows to appreciate the isolated and complementary influence of both microstructural effect types on the calculated Rietveld pattern. Now the effects of their simultaneous consideration of both approaches during the final steps of the refinement may be observed. The corresponding Rietveld plot, in Fig. 6, is very similar to that in Fig. 4. On the other hand, from Table 1 it can be assessed the better quality of this last refinement ($\chi^2 = 5{\cdot}09$). The phase abundances are now similar to those obtained after the consideration of just preferred orientation effects.

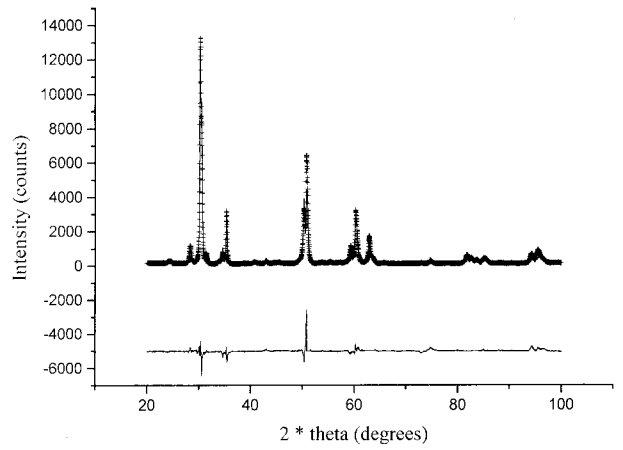

Fig. 5. Rietveld profile fit similar to that in Fig. 1, but including anisotropic broadening effects for the tetragonal phase.

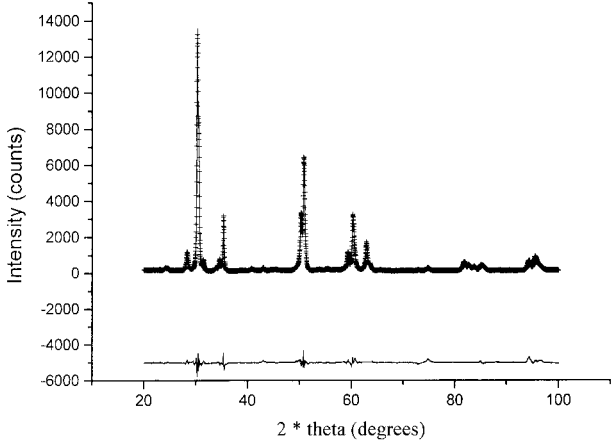

Fig. 6. Rietveld profile fit similar to that in Fig. 1, but including preferred orientation and anisotropic broadening effects for the tetragonal phase.

From the results just discussed, it is found that the omission of the preferred orientation correction during the refinement yields a transfer between tetragonal and monoclinic phases (those phases which have orientation relations within cubic matrix[16]). The overlooking of anisotropic broadening seems to be of secondary importance in relation to the quality of the refinement, but disregarding this effect causes a transfer between tetragonal and cubic phases. Finally, by using the BREADTH program[29] it has been determined the volume-weighted distribution of particle size for tetragonal precipitates. The program applies the 'double-Voigt' method,[30] which is equivalent to the Warren–Averbach approach.[31] Thus, by the choice of a reflection *hkl* of the pure profile and its harmonics, the program evaluates the column-length distribution normal to the (*hkl*) planes. In Fig. 7 it can be appreciated both lognormal distribution functions concerning the size of the precipitates along the rotation axis and within the habit plane. The averaged mean values are, respectively, 17 and 81 nm, which are consistent with an aspect ratio close to 5. TEM observations (see Fig. 2) indicates a larger disk diameter, about 100 nm. In any case it is thought that the agreement is good, and the differences probably arise because artifacts during the deconvolution process leading to the pure X-ray profile.

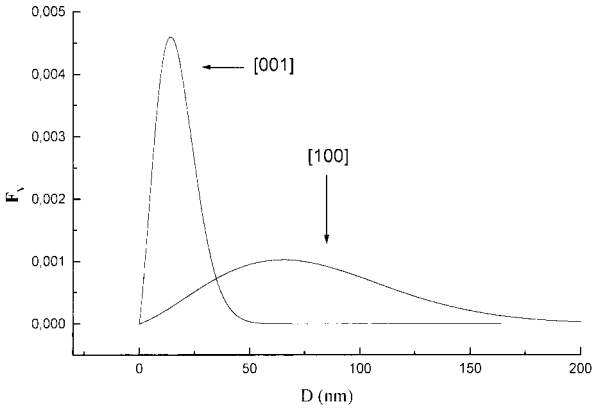

Fig. 7. Grain size distribution functions, F_v (D), for the tetragonal precipitates. The size of the precipitates is estimated along the directions corresponding to the rotation axis, [001], and within the habit plane, [100].

4 Conclusion

Nowadays the Rietveld refinement is probably the most reliable current method for doing quantitative phase analysis.[20] Multiple phases may be refined simultaneously and phase abundances be calculated from the separate overall scale factors. In some cases it is important to model some less usual effects, as preferred orientation and anisotropic broadening. It is shown that, for the studied peak-aged 9 mol% Mg-PSZ, the consideration of such effects for the tetragonal phase becomes necessary, not only in order to improve the refinement but also with the aim of obtaining accurate phase proportions. Success of the attempt here applied is aided by the fact that tetragonal phase is the majority one, then increasing the sensitivity of its microstructural effects. Finally, the calculated distribution functions of the tetragonal precipitate sizes were consistent with characteristic sizes deduced from TEM images.

Acknowledgements

The research was partly supported by the spanish CICYT under grants nos MAT94-043 and MAT94-0120-C03-02. One of the authors (R.F.) acknowledges a fellowship from the Instituto de Cooperación Iberoamericana (I.C.I.).

References

1. Hannink, R. H. and Swain, M. V., *Mat. Sci. Res.*, 1986, **20**., 259.
2. Hill, R. J., Howard, C. J. and Reichert, B. E., *Mat. Sci. Forum*, 1998, **34–36**, 159.
3. Kisi, E. H., Howard, C. J. and Hill, R. J., *J. Am. Ceram. Soc.*, 1989, **72**, 1757.
4. Hill, R. J. and Reichert, B. E., *J. Am. Ceram. Soc.*, 1990, **73**, 2822.
5. Howard, C. J., Kisi, E. H., Hill, R. J. and Roberts, R. D., *J. Am. Ceram. Soc.*, 1990, **73**, 2828.
6. Garvie, R. C. and Nicholson, E. S., *J. Am. Ceram. Soc.*, 1972, **55**, 303.
7. Evans, P. E., Stevens, R. and Binner, J. G., *Br. Ceram. Trans. J.*, 1984, **83**, 39.
8. Schmid, H. K., *J. Am. Ceram. Soc.*, 1987, **70**, 367.
9. Howard, C. J. and Kisi, E. H., *J. Am. Ceram. Soc.*, 1990, **73**, 3096.
10. Caracoche, M. C., Rivas, P. C., Pasquevich, A. F., López-García, A. R., Aglietti, E. and Scian, A., *J. Mat. Res.*, 1993, **8**, 605.

11. Sakuma, T. and Suto, H., In *Science and Technology of Zirconia III*, ed. S. Somiya, N. Yamamoto and H. Yanagida. *Advances in Ceramics*, 1988, **34**, 531.
12. Sugiyama, M. and Kubo, H., In *Science and Technology of Zirconia III*, ed. S. Somiya, N. Yamamoto and H. Yanagida. *Advances in Ceramics*, 1988, **34**, 965.
13. Chaim, R., Rühle, M. and Heuer, A. H., *J. Am. Ceram. Soc.*, 1985, **68**, 427.
14. Sánchez-Bajo, F., Cachadiña, I., Solier, J. D., Guiberteau, F. and Cumbrera, F. L., *J. Am. Ceram. Soc.*, 1997, **80**, 232.
15. Ikuma, Y., Sugiyama, T. and Okano, J., *J. Mat. Res.*, 1993, **8**, 2757.
16. Bansal, G. K. and Heuer, A. H., *J. Am. Ceram. Soc.*, 1975, **58**, 235.
17. Lanteri, V., Mitchel, T. E. and Heuer, A. H., *J. Am. Ceram. Soc.*, 1986, **69**, 564.
18. Khachaturyan, A. G., *Theory of Structural Transformations in Solids, 7, 8, 11*. Wiley, New York, 1983.
19. Rodriguez-Carvajal, J., FULLPROF: a program for Rietveld refinement and pattern matching analysis. In *Abstracts of the Satellite Meeting on Powder Diffraction of the XV Congress of the IUCr*, p. 127, Toulouse, France. Grenoble, France, 1990.
20. The Rietveld Method, ed. R. A. Young, ch. 1, In *IUCr Monographs on Crystallography*, Vol. 5. Oxford University Press, 1993.
21. Dollase, W. A., *J. Appl. Cryst.*, 1986, **19**, 267.
22. Caglioti, G., Paoletti, A. and Ricci, F. P., *Nucl. Instrum. Methods*, 1958, **3**, 223.
23. Langford, J. I., Loüer, D., Sonneveld E. J. and Visser, J. W., *Powder Diffract.*, 1986, **1**, 211.
24. Rodriguez-Carvajal, J., Fernández-Díaz, M. T. and Martínez, J. L., *J. Phys. Condens. Mater.*, 1991, **3**, 3215.
25. Lathabai, S. and Hannink, R. H., In *Science and Technology of Zirconia V*, ed. S. P. Badwal, M. J. Bannister and R. H. Hannink. Technomic, Lancaster, PA, 1993.
26. Hannink, R. H., *J. Mat. Sci.*, 1983, **18**, 457.
27. Hughan, R. R. and Hannink, R. H., *J. Am. Ceram. Soc.* 1986, **69**, 556.
28. Sim, S. M. and Stubican, V. S., *J. Am. Ceram. Soc.*, 1987, **70**, 521.
29. Balzar, D., *J. Res. Natl. Inst. Stand. Technol.*, 1993, **98**, 321.
30. Balzar, D. and Ledbetter, H., *J. Appl. Cryst.*, 1993, **26**, 97.
31. Warren, B. E. and Averbach, B. L., *J. Appl. Phys.*, 1950, **21**, 595.